Ceramics International **22** (1996) 15–22

0272-8842(95)00047-X
0272-8842/96/$15.00

Low-Temperature Sintering of Submicronic Randomly Oriented $Bi_4Ti_3O_{12}$ Materials

M. Villegas, C. Moure, J. F. Fernandez & P. Duran

Instituto de Cerámica y Vidrio (CSIC), Electroceramics Department, 28500 Arganda del Rey, Madrid, Spain

(Received 3 November 1994; accepted 6 April 1995)

Abstract: Ultrafine powders of $Bi_4Ti_3O_{12}$ with a narrow size distribution were prepared by the oxalate coprecipitation method. Compacts of the calcined powders were pressureless sintered at 850–1100°C in air, and the densification process was studied by non-isothermal and dilatometric experiments. A rapid densification (~98% of theoretical density) below 875°C took place, which was attributed to both an uniform pore-size distribution in the green starting compact and a rearrangement of particles. The development of platelike grains, the platelike colony formation, and a rapid grain growth decreased densification above 900°C. Microstructural development was studied and dielectric and electrical preliminary results are also given.

1 INTRODUCTION

The bismuth titanate $Bi_4Ti_3O_{12}$ belongs to the Aurivillius compounds family that can be represented by the general formula $(Bi_2O_2)^{2-}$ $(A_{m-1}B_mO_{3m+1})^{2+}$ in which A can be a monovalent (Na^+, K^+,...), divalent (Pb^{2+}, Ba^{2+},...) or trivalent (Bi^{3+}...) cation or a mixture of them, B represents Ti^{4+}, Nb^{5+}, Ta^{5+}, etc., and m can have values of 2, 3, 4,... In the particular case of $Bi_4Ti_3O_{12}$, $m = 3$, and its crystal structure can be described as formed by two $BiTiO_3$ unit cells of hypothetical perovskite structure interleaved with $Bi_2O_2^{2+}$ layers.[1] At room temperature, $Bi_4Ti_3O_{12}$ presents a monoclinic (C_{1h} = m) symmetry, but above the Curie temperature (~675°C) the symmetry becomes tetragonal (D_{4h} = 4mmm). The spontaneous polarization has a magnitude as high as 50 $\mu C/cm^2$ and lies in a direction tilted approximately 7° from the major crystal surface in a plane parallel to the monoclinic b_o–c_o plane. The polarization along the c_o direction, after applying an electric field on the major crystal surface, yielded values of approximately 4 $\mu C/cm^2$.[2–3] The piezoelectric coefficient is also relatively high in these directions. These characteristics suggest $Bi_4Ti_3O_{12}$ to be an interesting piezoelectric ceramic for high-temperature applications.

As reported by several authors[4–8] optimized piezoelectric properties are achieved by almost complete alignment of the platelike bismuth titanate particles, and different techniques such as tape casting, hot-pressing and hot-forging were used to obtain well-oriented grain $Bi_4Ti_3O_{12}$ materials.[9–12] However, a problem with these bismuth titanate-based ceramics is their high electrical conductivity anisotropy, which is maximum in the basal plane.[6,9] Such an anisotropy increases with temperature and reaches a maximum near the transition temperature in $Bi_4Ti_3O_{12}$ single crystals.[13] Both the piezoelectric properties and the electrical conductivity being maximum along the same directions, a well-oriented grain $Bi_4Ti_3O_{12}$ ceramic material could be unsuitable for high-temperature applications.

The mechanism of electrical conductivity seems to be associated with the presence of oxygen defects in the form of anionic vacancies in the $Bi_2O_2^{2+}$ layers.[14] Consequently, an increase in the resistivity of these ceramics could be obtained in well-densified $Bi_4Ti_3O_{12}$ ceramics, with randomly

oriented small grain size to limit the conductivity along the $Bi_2O_2^{2+}$ layers.

The present work deals with the preparation of submicronic $Bi_4Ti_3O_{12}$ powders by the oxalate coprecipitation method, and sintered $Bi_4Ti_3O_{12}$ ceramics with a fine-grained microstructure. Some preliminary dielectric and electrical conductivity measurements were also carried out.

2 EXPERIMENTAL PROCEDURE

In order to obtain sub-micron $Bi_4Ti_3O_{12}$ powders, the oxalate coprecipitation method was used. Titanium tetrabutoxide $Ti(C_4H_gO)_4{\cdot}C_4H_9OH$ and $Bi(NO_3)_3 \cdot 5H_2O$ were used as TiO_2 and Bi_2O_3 oxide precursors, respectively. The appropriate amounts of both precursors were dissolved in a slightly acid isopropyl alcohol solution and then were added dropwise to a 0·3 M aqueous oxalic acid solution. A good coprecipitation of the oxalates was achieved by a careful pH control, and a small amount of aqueous $(NH_4)OH$ was added at the end of the coprecipitation process. The coprecipitate was thoroughly washed with isopropanol until an amorphous powder was obtained. After drying, the powder was calcined at 750°C for 1 h and attrition milled for 2 h in an isopropanol medium. The calcined powder was granulated and isostatically pressed at 200 MPa. The compacts were sintered at 850–1100°C for 2 h. The densification process was also studied by dilatometry in a dilatometer (Dl-24 Adamel-L'homargi).

Both the coprecipitated and the calcined powders were characterized by specific surface area measurements by using the BET method with nitrogen as the adsorbate (Micromeritics Accusorb 2100E),

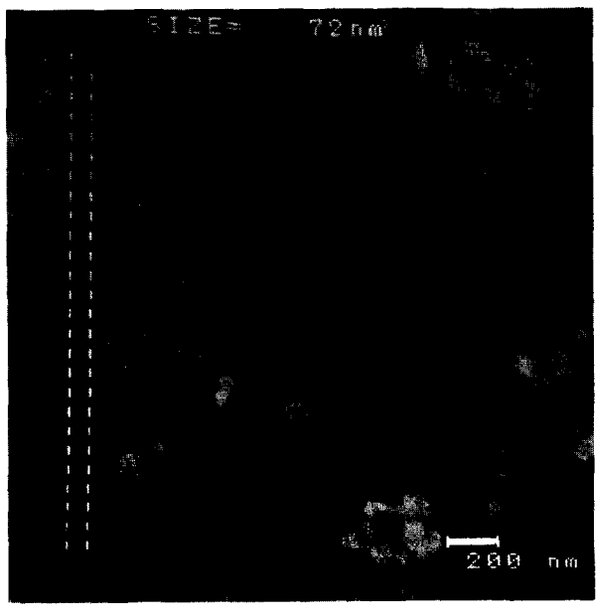

Fig. 1. Coprecipitate oxalate BIT powder.

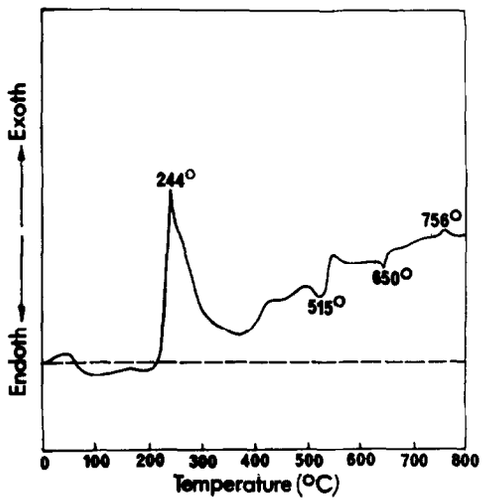

Fig. 2. DTA curve of BIT powder.

a particle size analyzer (Coulter LS 130), a differential thermal analyzer (STA409 Nescht), an X-ray diffractometer (D-5000 Siemens), and a scanning electron microscope (DSM950 Karl Zeiss).

The density of the sintered compacts was measured by the Archimedes method with water, and the pore size distribution and the pore volume in the green compacts were measured by mercury porosimetry using a porosimeter (Micromeritics Autopore II 9215). The microstructure of both the green and the sintered compacts was studied by SEM.

Dielectric and electrical characterization was carried out by using an HP-4192A impedance analyzer in the temperature range of 25°C–700°C at a frequency of 1 MHz.

The $Bi_4Ti_3O_{12}$ powder obtained by this method will be referred to as BIT.

3 RESULTS

3.1 Powder characteristics

As shown in the micrograph of Fig. 1, the coprecipitated BIT powder was formed by agglomerates of particles with size less than 50 nm and a specific surface of 25 m^2g^{-1} as determined by BET. Differential thermal analysis of this powder showed two exothermic effects at 244°C and 756°C, and two endothermic ones at 515°C and 650°C (see Fig. 2). The first exothermic effect, between 200 and 400°C, was due to both the combustion of the residual isopropanol, and the oxalate decomposition. At this temperature interval the main weight loss of the coprecipitate took place. The second exothermic effect could be due to the formation of the $Bi_4Ti_3O_{12}$ compound. The two endothermic effects were due to the loss of

Fig. 3. SEM of BIT calcined powder (bar = 1 μm).

some hydroxyl groups and the α–β transformation of an incipient formed $Bi_4Ti_3O_{12}$, respectively.

After calcining and attrition milling, BIT powders consisted of small and soft agglomerates of almost equiaxial shaped particles with ultimate average particle size less than 0·6 μm (see Fig. 3). The specific surface of the BIT powders was 2 m^2g^{-1}. The XRD analysis of the powders calcined at different temperatures, as shown in Fig. 4, indicated that $Bi_4Ti_3O_{12}$ starts to be formed below 550°C and the formation reaction is completed between 700 and 750°C in agreement with the DTA results. No other phases were detected. Apparently neither platelets nor needle-like particles were developed during the calcination of the powders. After compaction, the density of the green compacts was 55% of the theoretical one, and the pore size distribution curve, as shown in Fig. 5, showed an almost single and narrow pore-size distribution with an average pore diameter of 0·1 μm.

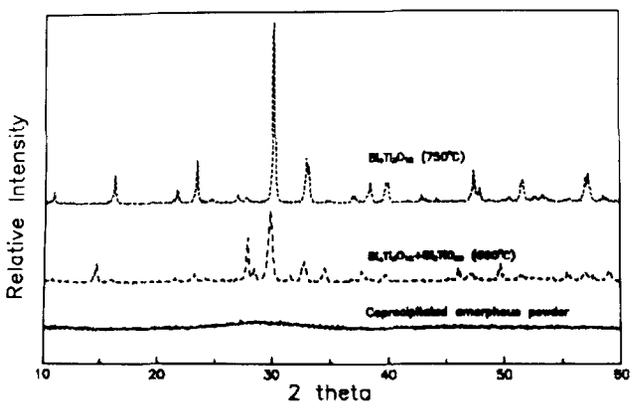

Fig. 4. XRD patterns of BIT powders calcined at different temperatures.

3.2 Sintering

Green compacts of BIT powder were fired at 850–1100°C for 2 h. Figure 6 shows the effect of sintering

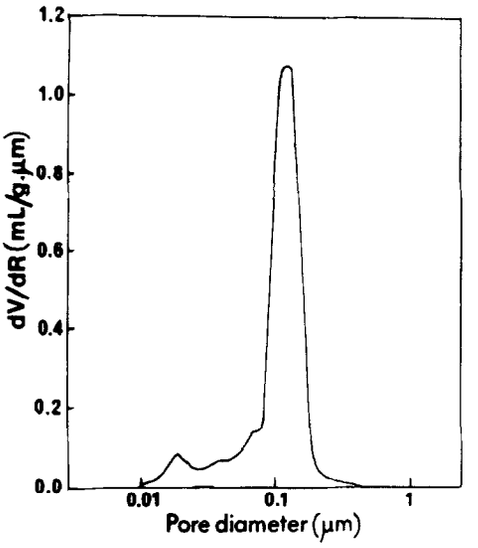

Fig. 5. Pore-size distribution in BIT green compacts.

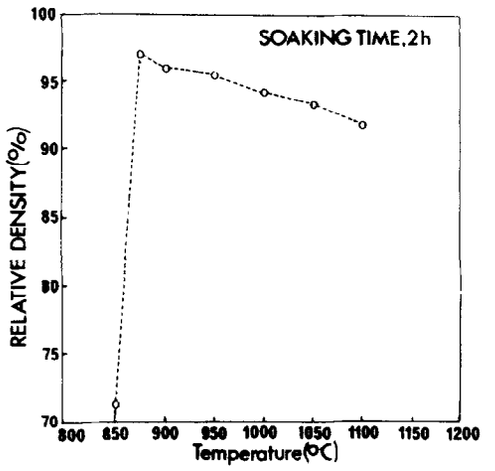

Fig. 6. Densification behavior of BIT compacts.

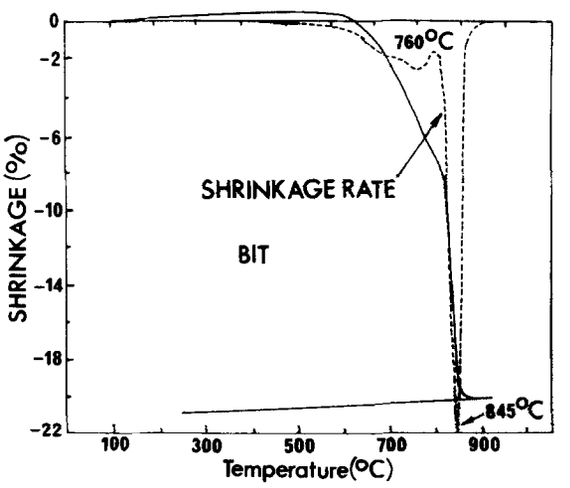

Fig. 7. Shrinkage and shrinkage rate curves of BIT compacts.

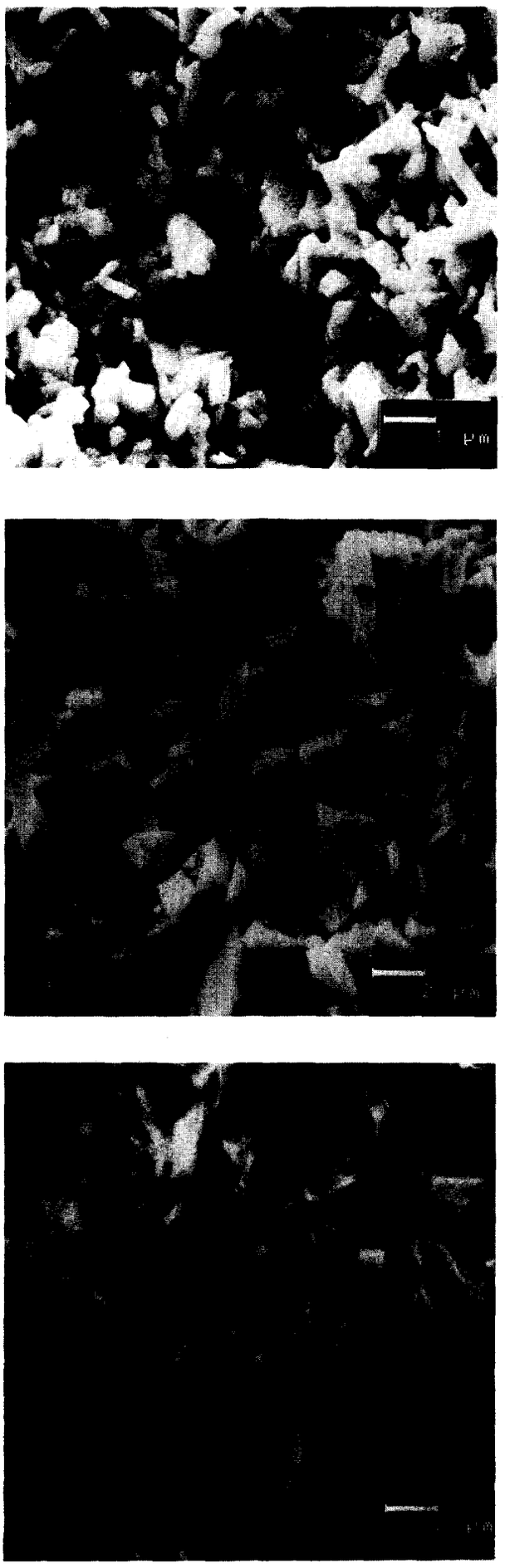

Fig. 8. Fracture surface of BIT samples sintered at (A) 850°C, (B) 875°C, and (C) 900°C.

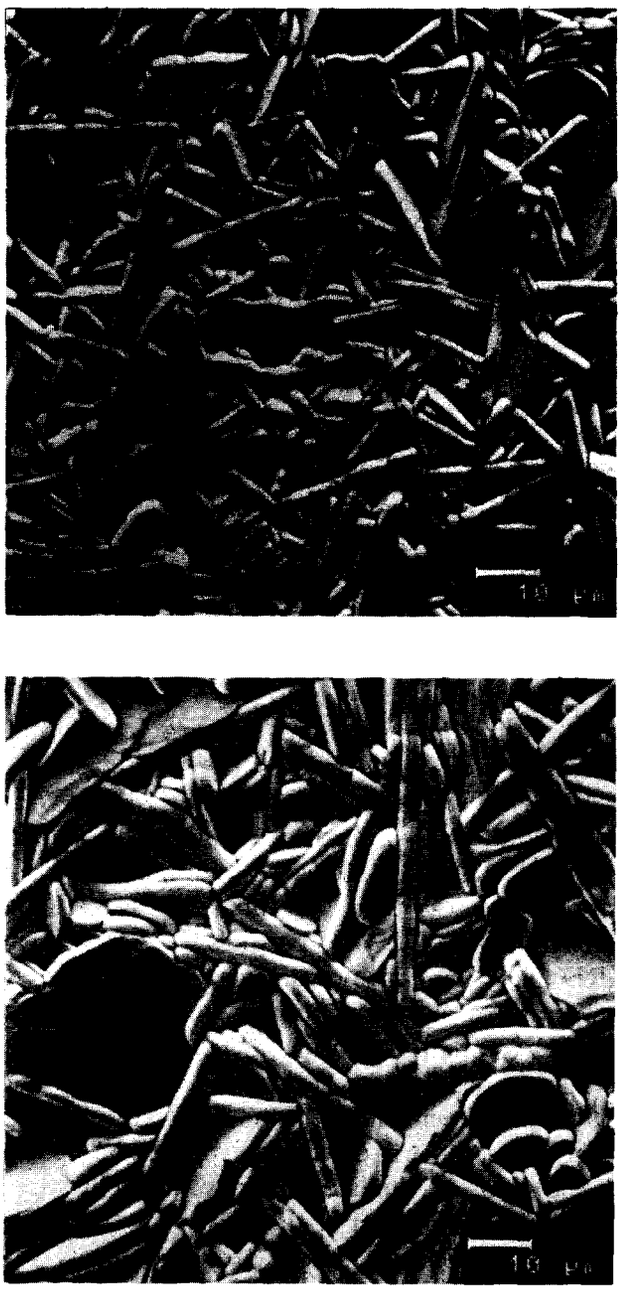

Fig. 9. Microstructure of polished and thermally etched BIT samples sintered at (A) 1050°C and (B) 1100°C.

temperature on the densification of powder compacts. The maximum density was achieved for a sintering temperature of 875°C. The densification of BIT compacts took place rapidly in a narrow temperature interval, between 850 and 875°C, above this temperature, the density decreased slightly.

The densification process was also studied by constant rate heating (CRH) experiments. As shown in Fig. 7, BIT compact started to shrink at a temperature as low as 600°C and an endpoint was reached at 875°C for a shrinkage of about 21%. The shrinkage rate curve showed two maxima, at about 760°C and 845°C. Above those temperatures the shrinkage rate slightly decreased.

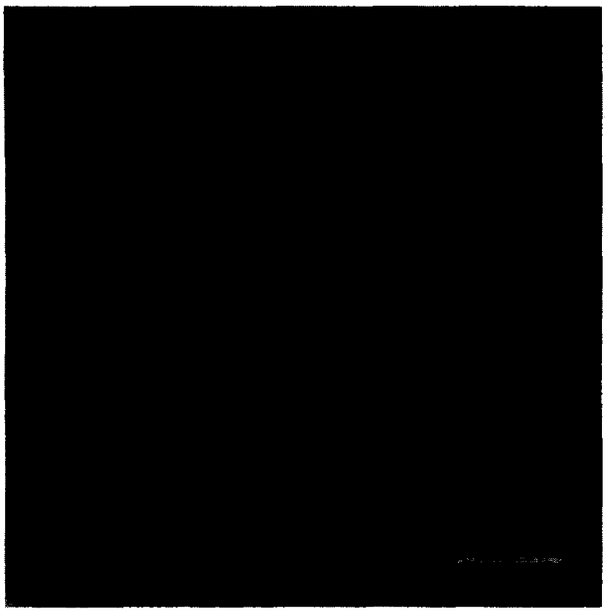

Fig. 10. Bloating phenomenon in BIT samples sintered at 1100°C.

3.3 Microstructural development

Figure 8 shows the fracture surface of BIT samples sintered at 850, 875 and 900°C. At the lower temperature, randomly oriented grains with some developed platelike structures or needles were observed. The porosity was mainly located on grain boundaries, and no pores were located in the interior of the grains and/or platelike structures. The grain size, less than 1 μm, indicated that no appreciable grain growth was produced at this sintering temperature. In the sample sintered at 875°C, there was a rearrangement of both grains and small platelikes, and porosity almost disappeared. This rearrangement coincided with the maximum of the density reached at this temperature (see Fig. 6). The few developed platelikes were ~0·5 μm thick and ~2 μm diameter. With further increase in temperature, many spherical pores were developed, and a rapid grain growth in the sample sintered at 900°C was observed. Thus, the platelikes were ~1 μm thick and ~5 μm diameter. At higher temperatures some spherical pores located at the interior of the platelikes and non-spherical or triangular pores located between them were observed. As a consequence, many cracks were also produced which, therefore, lead to a decrease in density. Figure 9 (A) and (B) shows the microstructure of the BIT polished and thermally etched surfaces of samples sintered at 1050 and 1100°C. It can be mentioned that a bloating phenomenon was observed in some BIT samples sintered above 900°C as shown in Fig. 10 (A) and (B).

3.4 Dielectric properties

Dielectric constant of BIT sintered samples was measured at room temperature. Depending on the sintering temperature, the dielectric constant values ranged from 140 to 180, which indicated some influence of the grain size. Figure 11 shows the temperature dependence of the dielectric constant of $Bi_4Ti_3O_{12}$. The dielectric constant increases with temperature, reaches a peak of about 1500 at 680°C, then decreases according to the Curie–Weiss law. In all cases a shoulder is present at lower temperatures (~500°C). The bulk conductivity measured at 100°C is $9{\cdot}3 \times 10^{-9}$ $(\Omega.cm)^{-1}$ and $7{\cdot}8 \times 10^{-6}$ $(\Omega.cm)^{-1}$ at 250°C.

4 DISCUSSION

The sintering behavior of BIT compacts strongly depends on the morphology of the $Bi_4Ti_3O_{12}$ particles.

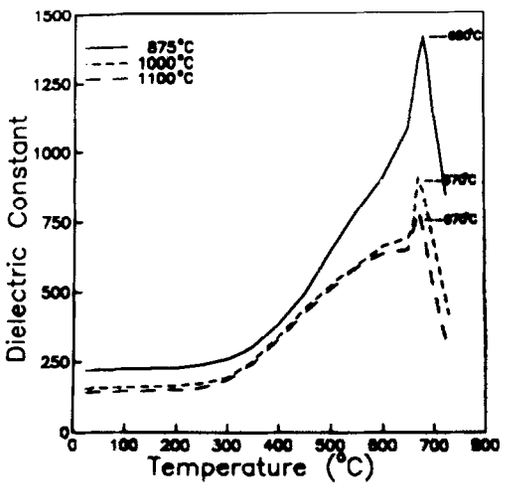

Fig. 11. Dielectric constant of BIT sintered samples vs temperature.

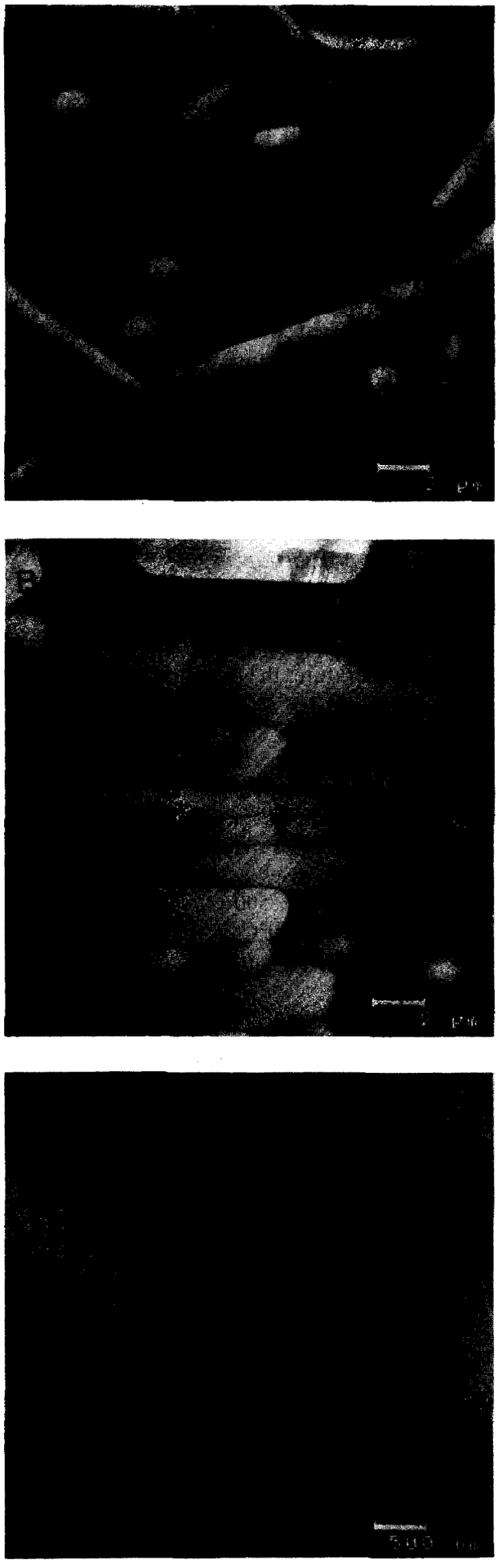

Fig. 12. Grain growth process in BIT sintered samples.

Thus, sintering behavior of BIT powder with almost equiaxial particles was quite different from that with platelike particles.[15] In all cases, the calcined powders were formed of soft agglomerates of different sizes and shapes but the primary particle was smaller than 1 μm (see Fig. 3). In spite of the relatively low green density, the BIT compacts densified at a temperature lower than that reported for conventional BIT powders.[15] Thus, a maximum density of ~98% was achieved at 875°C (Fig. 6), whereas ~90% density was reported at a temperature as high as 1150°C for platelike BIT powders.[15] A rapid densification occurred above 850°C in a temperature interval as narrow as 25°C in coprecipitated oxalate BIT powders contrary to a rather slow densification process found in conventional BIT powders.[8,15] For higher temperatures, the density slightly decreased in both cases. The rapid densification can be attributed to the very uniform pore-size distribution in the green starting compacts (Fig. 5). The steep shrinkage curve, as shown in Fig. 7, could also support such a statement.[16] On the other hand, the initial rearrangement of particles at 875°C can also contribute to the fast densification, as reported by Chazono *et al.*[17] in the case of the sintering of platelike $Bi_4Ti_3O_{12}$ powders. Finally, although no liquid phase formation was detected at 875°C, one can think that small deviations from the stoichiometric $Bi_4Ti_3O_{12}$ composition could be present and, if this is so, then the presence of a very small transient liquid amount would coexist with the $Bi_4Ti_3O_{12}$ compound above 860°C according to the phase diagram of the Bi_2O_3–TiO_2 system.[18] Such a small amount of transient liquid would also enhance the densification process. A deeper study, now in progress, of the microstructure by TEM will help to elucidate whether this is true.

As presented in Fig. 9, two maxima in the shrinkage rate curves were registered, and the temperature difference between them was 85°C. At the first, lower, temperature maximum, 760°C, the density of the sintered samples was less than 70% of theoretical and sintering can be attributed to the porosity migration from the intra-agglomerates to the inter-agglomerates pores. At this first stage, the finer porosity was eliminated and an increase of the volume of pores between agglomerates with a slight densification took place. Above this temperature, a slight decrease in the shrinkage rate occurred, followed by a rapid increase in the shrinkage rate between 800 and 845°C. Such an increase in the shrinkage rate indicated a rapid elimination of the interagglomerate pores and agreed well with the maximum of the density found in the isothermal sintering experiments (see

Fig. 6). These facts along with the principally transgranular fracture of the sample sintered at 875°C, as shown in Fig. 8, could be corroboration of a combined effect of at least two factors in enhancing densification, (a) extremely uniform pore-size distribution, and (b) rearrangement of particles. On the other hand, no exaggerated grain growth was observed up to 875°C, but above that temperature a rapid platelike and platelike colony formation, as well as grain growth with the generation of an additional porosity, occurred (see Fig. 9). The shape of the pores generated, as shown in Fig. 10 (A) and (B), leads us to assume that a rapid gas loss (vaporized bismuth oxide, oxygen or both) could be occurring at high temperature. Such an additional porosity and the cracks produced as a consequence of the platelike grain growth led to a decrease in the density. On the other hand, at high temperature (> 900°C) the activity of bismuth oxide is considerable, and then some dissociation phenomenon with oxygen rejection could take place. Such an oxygen rejection leads to both the observed bloating phenomenon and a probable oxygen enrichment at the grain boundaries as reported by Jovalekic *et al.*[19] If this is so, then it could be due to bismuth reduction to a suboxide state, giving rise to the generation of oxygen vacancies which would be located in the vicinity of bismuth cations inside the $Bi_2O_2^{2+}$ layer. The oxygen vacancies would thus be responsible for the abnormally high bulk conductivity of BIT samples.

Above 900°C the grain growth process takes place by changing the shape of the equiaxial particles to platelike grains and, as the temperature increases, the formed platelike grains grow in an uncontrollable manner to larger platelike ones by both grain boundary diffusion and by face-to-face interaction (see Fig. 12 (A), (B) and (C)) and then the grain growth carries on at the expense of the smaller grains. The grain growth rate determines in a great measure the pore location at the grain boundaries or within the grains. Brooks and Damijanovic[20] recently reported a possible way for controlling the microstructure of BIT-based ceramics using some additives.

Dielectric permittivity measurements carried out in the denser BIT sintered samples at room temperature showed a relative dispersion of the dielectric constant values as a function of the sintering temperature which indicates the influence of both the grain size and the oxygen defects concentration.[13] This being so, then the relatively high bulk conductivity of the BIT sintered samples could corroborate such a statement. The presence of a bump below the ferroelectric–paraelectric transition temperature is not well known, and further experiments are now in progress to understand such a phenomenon better.

5 CONCLUSIONS

Randomly oriented ceramics were fabricated by sintering $Bi_4Ti_3O_{12}$ submicronic particles obtained by an oxalate coprecipitation method. The formation of very small and soft agglomerates of almost equiaxial-shaped particles favoured both the compaction and the densification process and, thus, high density (~98% theoretical) was achieved at a temperature as low as 875°C. From the results obtained, it is assumed that a combined effect of both the very uniform pore-size distribution in the green starting compacts, and the rearrangement of particles enhanced the densification of oxalate $Bi_4Ti_3O_{12}$ prepared powders above 850°C. An exaggerated and uncontrollable grain growth with randomly oriented platelike grains, above the maximum densification temperature, was responsible for the decrease in sintered density. In spite of the high density of the BIT sintered samples, a relatively high dispersion in the dielectric constant values and an abnormally high electrical conductivity were found. These results seem to indicate a strong influence of the grain size and, as a consequence, it is suggested to carry out a careful study of the following steps: (a) better control of starting raw materials; (b) different sintering schedules; and (c) doping, if necessary, for controlling exaggerated grain growth.

REFERENCES

1. AURIVILLIUS, B., Mixed bismuth oxides with layer lattices. *Arkiv for Kemi*, **1** (1949) 499.
2. DORRIAN, J. I., NEWNHAM, R. E. & SMITH, D. K., Crystal structure of $Bi_4Ti_3O_{12}$ *Ferroelectrics*, **3** (1971) 17.
3. TAYLOR, G. W., KENEMAN, S. A. & MILLER, A., Depoling of single domain bismuth titanate. *Ferroelectrics*, **2** (1971) 11.
4. SHOJI, K. & UEHARA, Y., Grain orientation of $Bi_4Ti_3O_{12}$ ceramics by cold uniaxial method. *Japan. J. Appl. Phys*, **22**, Supplement 22-2 (1983) 50.
5. TAKENAKA, T. & SAKATA, K., Pyroelectric properties of grain-oriented bismuth layer structured ferroelectric ceramics. *Japan. J. Appl. Phys.*, **22**, Supplement 22-2 (1983) 53.
6. TAKENAKA, T. & SAKATA, K., Grain orientation effects on electrical properties of bismuth layer-structured ferroelectric $Pb_{1-x}(NaCe)_{x/2}Bi_4Ti_4O_{15}$ solid solution. *J Appl. Phys.*, **55** (1984) 1092.
7. TAKENAKA, T., SAKATA, K. & TODA, K., Piezoelectric properties of bismuth layer-structured ferroelectric $Na_{0.5}Bi_{4.5}Ti_4O_{15}$ ceramic. *Japan. J Appl. Phys.*, **24**, Supplement 24-2 (1985) 730.
8. INOUE, Y., KIMURA, T. & YAMAGUCHI, T., Sintering of platelike bismuth titanate powders. *Am. Ceram. Soc. Bull.*, **62** (1983) 704

9. INOUE, Y., KIMURA, T., YAMAGUCHI, T., NAGATA, K. & OKAZAKI, K., Grain orientation and electrical properties of hot-pressed bismuth titanate ceramics. *Yogyo-Kiokai-Shi*, **92** (1984) 416.
10. WATANABE, H., KIMURA, T. & YAMAGUCHI, T., Particle orientation during tape casting in the fabrication of grain-oriented bismuth titanate. *J. Am. Ceram. Soc.*, **72** (1989) 289.
11. TAKENAKA, T., SHOJI, K., TAKAI, H. & SAKATA, K., Ferroelectric and dielectric properties of press forged bismuth titanate ceramics. *Proc. 19th Japan Congress on Materials Research*, Tokyo, Japan, March 1976, pp. 230–3.
12. WATANABE, H., KIMURA, T. & YAMAGUCHI, T., Sintering of platelike bismuth titanate powder compacts with preferred orientation. *J. Am. Ceram. Soc.*, **74** (1991) 139.
13. FONSKOVA, A. & CROSS, L. E., Dielectric properties of bismuth titanate. *J. Appl. Phys.*, **41** (1970) 2834.
14. SINJAKOV, E. V., DUDNIK, E. F., DUDA, V. M., PODOLSKI, V. A. & GORFUNKEL, M. A., Relaksaciya dielectrichescoi pronicaemosti vismuta. *Fizika Tverdogo Tela*, **16** (1974) 1515.
15. CHAZONO, H., KIMURA, T. & YAMAGUCHI, T., Fabrication of grain-oriented $Bi_4Ti_3O_{12}$ ceramics by normal sintering — I. Tapecasting and sintering. *Yogyo-Kiokai-Shi*, **93** (1985) 485.
16. PERANSKAYA, E. I., REZ, I. S., KOZLOVA, L. V., SKORIKOV, V. M. & SLAVOV, V. I., Phase diagram of the Bi_2O_3–TiO_2 system. *Izv. Akad. Nauk SSSR, Neorgan. Materialz.*, **1** (1965) 232.
17. YAMAGUCHI, T. & KOSHA, H., Sintering of acicular Fe_2O_3 powder. *J. Am. Ceram. Soc.*, **5** (1981) C-84.
18. CHAZONO, H., KIMURA, T. & YAMAGUCHI, T., Fabrication of grain-oriented $Bi_4Ti_3O_{12}$ ceramics by normal sintering — II. Sintering mechanism. *Yogyo-Kiokai-Shi*, **94** (1986) 324.
19. JOVALEKIC, J., ATANASOSKA, L., PETROVIC, V. & RISTIC, M. M., The influence of thermal treatment on polarization behavior of $Bi_4Ti_3O_{12}$ ceramics. In *Science of Sintering*, ed. D. P. Uskokovic *et al.* Plenum Press, New York, 1989, p. 545.
20. BROOKS, H. S. & DAMIJANOVIC, D., Microstructural control of bismuth titanate based ceramics. In *Third ECERS*, vol. 2, ed. P. Durán & J. F. Fernández. Faenza Edit. Iber., Madrid, 1993, p. 199.